

Artificial swimmers in concentration gradients: Simulation and learning

Gustavo C. Buscaglia¹, Stevens Paz², Roberto F. Ausas¹, Juan P. Carbajal³

¹*Instituto de Ciências Matemáticas e de Computação, Universidade de São Paulo
São Carlos, Brazil*

gustavo.buscaglia@icmc.usp.br, rfausas@icmc.usp.br

²*Departamento de Matemáticas, Universidad del Valle*

Calle 13 No. 100-00, Cali, Colombia

stevens.paz@correounivalle.edu.co

³*Ostschweizer Fachhochschule, Institut für Energietechnik IET*

Rapperswil, Switzerland

juanpablo.carbajal@ost.ch

Abstract. The coupled problem of hydrodynamics and solute transport for artificial microswimmers is studied, with the Reynolds number set to zero and Péclet numbers (Pe) ranging from 0 to 100. The adopted method is the numerical simulation of the problem with a finite element code based upon the FEniCS library. Details of the second-order treatment of the time-evolving geometry are presented and shown to be essential for the basic physics to be respected. The code is first applied to compute the effective solute intake of several artificial swimmers as functions of the Péclet number. The results confirm that no significant gain in solute intake is achieved by swimming if Pe is smaller than 10. We also consider the swimmers as learning agents inside a fluid that has a concentration gradient in the far field. We couple the simulations with reinforcement learning processes and investigate the ability of the agents to learn to move towards the region of higher concentration. The results demonstrate that microscopic organisms need to solve a challenging learning problem to migrate efficiently when exposed to chemical inhomogeneities.

Keywords: Fluid-structure interaction, Solute transport, Learning, Microswimmer.

1 Introduction

Locomotion and transport phenomena are essential in microbiology, and have attracted the interest of pioneers of Fluid Mechanics such as Taylor [1], Lighthill [2] and Purcell [3], among others. Comprehensive reviews have been made available by Elgeti et al. [4], Lauga [5] and Goldstein [6, 7].

To understand the fundamental mechanisms of movement and chemical exchange at the microbial scale, it is useful to analyze simplified models of microswimmers. Such is the case of the *squirmers*, a model consisting of a single spheroidal particle with a given slip velocity over its surface that mimics the net effect of a ciliary layer (see Lighthill [8] and Blake [9]). The locomotion of squirmers is by now fairly well understood, and the transport of a chemical species to/from its surface has been thoroughly studied by Magar et al. [10] and Magar and Pedley [11].

The squirmer model adapts well to micro-swimmers that move by ciliary action, such as the Paramecium or the Opalina. Other swimmers, however, generate thrust by rearranging their body parts so as to perform a *swimming gait*. Simplified models for such swimmers typically consist of several rigid bodies which are connected by extensible rods or by angular joints. A typical example is the rectilinear three-sphere swimmer, introduced by Najafi and Golestanian [12, 13] and more recently studied by Nasouri et al. [14] and Berti [15]. There exist other simplified models of micro-swimmers (see Pak et al. [16], Cohen and Boyle [17] and Wang and Othmer [18]), such as the push-me-pull-you, rotating variants of the three-sphere swimmer, and articulated snake-like models inspired in Taylor's swimming sheet.

For these multi-body swimmers the hydrodynamics is more complex due to the significant shape variations. Their locomotion is only partially understood, having mainly been studied by asymptotic approximations. Here we present a more realistic analysis, in which the swimmer interacts with a Stokes fluid with accurate consideration of the geometry and boundary conditions. For this purpose we use an in-house code based on the FEniCS package [19], adapted from those used by Paz and Buscaglia [20] and Ausas et al. [21].

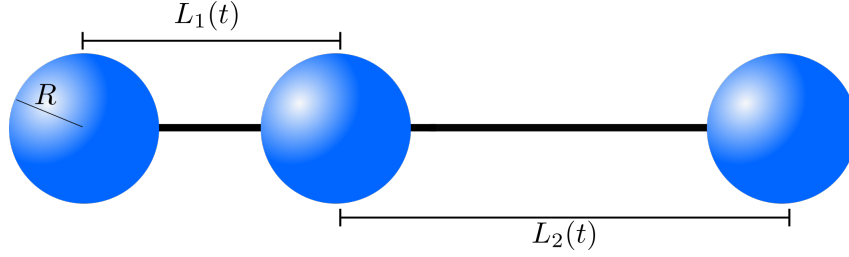


Figure 1. Rectilinear three-sphere swimmer introduced by Najafi and Golestanian [12].

Further, we numerically solve not just the locomotion of multi-body swimmers but also the associated solute transport and mass transfer problem. To our knowledge, the only published work with a comparable approach is due to Tam and Hosoi [22] (for a case of a flagellated sphere). It is clear that micro-organisms depend on solute transport for their subsistence, where the solute may be a nutrient to be absorbed or waste to be shed.

We present here some examples of two types of analyses. The first type corresponds to the simulation of a specified swimming gait, quantitatively evaluating the effect of locomotion on mass transfer. Then we turn to *learning* analyses, in which the decisions about the swimmer's movements are taken algorithmically. These analyses aim to determine efficient sequences of movements by the Q-learning method.

2 The simulation problem: fluid-solid interaction with transport

The Najafi-Golestanian swimmer [12] consists of three spheres of radius R , joined by two contractible arms of negligible thickness, as shown in Fig. 1. We denote by $\mathcal{B} = \cup_{i=1}^3 \mathcal{B}_i$ the domain occupied by the swimmer, being \mathcal{B}_i the i -th sphere. The time dependent length of the arms, $L_1(t)$ and $L_2(t)$, are given. The configuration at any time t is totally determined by $X(t)$, $L_1(t)$ and $L_2(t)$, since

$$X_1 = X - \frac{2L_1}{3} - \frac{L_2}{3}, \quad X_2 = X + \frac{L_1}{3} - \frac{L_2}{3}, \quad X_3 = X + \frac{L_1}{3} + \frac{2L_2}{3},$$

where X_1 (left sphere), X_2 (central sphere) and X_3 (right sphere) are the positions of the sphere's centers, and X is the centroid of the whole swimmer.

The domain of the incompressible Newtonian fluid that surrounds the swimmer is denoted as $\Omega_f = \Omega \setminus \mathcal{B}$, where Ω is a large domain representing an infinite medium, and its Cauchy stress tensor is given by

$$\boldsymbol{\sigma} = -p\mathbf{I} + \mu (\nabla \mathbf{u} + \nabla \mathbf{u}^T),$$

where μ , \mathbf{u} and p denote the viscosity, the velocity and the pressure of the fluid, respectively, and \mathbf{I} is the identity matrix. The interaction problem reads: *Given $X(0)$, $L_1(t)$ and $L_2(t)$, for $t > 0$ find $X(t)$, $\mathbf{u}(\mathbf{x}, t)$ and $p(\mathbf{x}, t)$ such that*

$$\nabla \cdot \boldsymbol{\sigma} = \mathbf{0}, \quad \text{in } \Omega_f, \quad (1)$$

$$\nabla \cdot \mathbf{u} = 0, \quad \text{in } \Omega_f, \quad (2)$$

$$\int_{\partial \mathcal{B}} \boldsymbol{\sigma} \cdot \hat{\mathbf{n}} dS = \mathbf{0}, \quad (3)$$

$$\mathbf{u} = \left(\frac{dX}{dt} - \frac{2}{3} \frac{dL_1}{dt} - \frac{1}{3} \frac{dL_2}{dt} \right) \hat{\mathbf{e}}, \quad \text{on } \partial \mathcal{B}_1, \quad (4)$$

$$\mathbf{u} = \left(\frac{dX}{dt} + \frac{1}{3} \frac{dL_1}{dt} - \frac{1}{3} \frac{dL_2}{dt} \right) \hat{\mathbf{e}}, \quad \text{on } \partial \mathcal{B}_2, \quad (5)$$

$$\mathbf{u} = \left(\frac{dX}{dt} + \frac{1}{3} \frac{dL_1}{dt} + \frac{2}{3} \frac{dL_2}{dt} \right) \hat{\mathbf{e}}, \quad \text{on } \partial \mathcal{B}_3. \quad (6)$$

The Stokes problem corresponds to Eqs. (1) and (2), Eq. (3) represents the force-free condition over the swimmer and Eqs. (4)-(6) impose the no-slip condition at the surface of the spheres. Here, $\hat{\mathbf{n}}$ is the unit normal outwards of Ω_f and $\hat{\mathbf{e}}$ the unit positive direction of motion.

The structure of the mathematical problem is the same of other swimmer models, as discussed by Alouges [23]. There exist some *shape variables* ξ that are given (or controlled), which in this case are L_1 and L_2 . There also exist *position variables* \mathbf{p} that determine the position and orientation of the swimmer as a whole. In the rectilinear

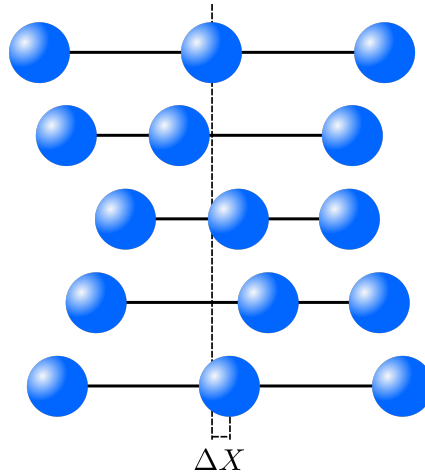


Figure 2. Swimming gait for the three-spheres swimmer considered by Najafi and Golestanian [12]. X_1 , X_2 and X_3 are the positions of the centers of the left, central and right spheres, respectively.

swimmer above it is simply $\mathbf{p} = X$ (this is, a scalar variable), but \mathbf{p} in general parameterizes arbitrary rotations and translations. The state of the swimmer is given by $\mathbf{q} = (\mathbf{p}, \xi)$. The instantaneous velocity field of the swimmer is linear in ξ , as is $\dot{\mathbf{p}}$.

A non-zero net displacement is achieved by the swimmer when a non time reversible sequence of arm movements are performed. We consider a simplified version of the movements consisting on the activation of one arm at a time, going from fully extended, with maximum arm length W , to fully contracted, with minimum arm length $W - w$. The resulting swimming gait then induces an advancing distance ΔX per gait, as shown in Fig. 2.

We suppose that a solute concentration field C , with diffusivity D , is transported by the fluid velocity field around the swimmer. The problem for C reads: *Given the initial solute distribution $C(\mathbf{x}, t = 0)$, find $C(\mathbf{x}, t)$, for $t > 0$, satisfying*

$$\frac{\partial C}{\partial t} + \mathbf{u} \cdot \nabla C - D \nabla^2 C = 0, \quad \text{in } \Omega_f, \quad (7)$$

$$C = 0, \quad \text{on } \partial \mathcal{B}_i, \quad (8)$$

with boundary conditions $C = C_\infty$ far away from the swimmer.

The total solute flux J to the swimmer is defined as

$$J(t) = \int_{\partial \mathcal{B}(t)} D \nabla C \cdot \hat{\mathbf{n}} \, dS. \quad (9)$$

The fluid-solid interaction problem is numerically solved by P_1 conforming GLS-stabilized finite elements for velocity and pressure, and P_2 for the concentration variable, using the FEniCS package [19]. An elasticity problem is solved for the moving mesh which is complemented by a regular remeshing that depends on the quality of the mesh. The time stepping strategy for the hydrodynamic problem follows a second-order predictor-corrector method, and a second-order trapezoidal scheme is used for the solute transport.

3 The effect of swimming on the solute intake

In the optimal swimming gait presented by Najafi and Golestanian [12], and shown in Fig. 2, the velocity S of contraction and extension of the arms is constant, so, the duration of the gait is $T = 4w/S$, which is the time it takes the swimmer to recover its initial posture with a translation of size ΔX .

After some development time \mathcal{T} , the concentration field reaches a periodic evolution in the swimmer's frame, this is, for $t > \mathcal{T}$, $C(\mathbf{x} + \Delta \mathbf{X}, t + T) = C(\mathbf{x}, t)$, implying that $J(t)$ is periodic, $J(t + T) = J(t)$. We define as $J_s(\text{Pe})$ the average solute flux when the swimmer is executing the swimming gait, with Péclet number $\text{Pe} = \frac{SR}{D}$, and J_0 the steady diffusive flux toward the three-sphere swimmer when its arms are totally extended. The solution of the full hydrodynamic and transport problem yields the average Sherwood number J_s/J_0 as a function of Pe for each case, as shown in Fig. 3. It is worth pointing out that for very low Pe the solute flux is maximal when the swimmer is immobile with both arms extended, which can also be seen as $w = 0$. The swimming gait takes the arms out of the optimal position and thus results in $J_s < J_0$, as evinced by Fig. 3 for $\text{Pe} < 5$.

Clearly, executing the swimming gait is only favorable at high Pe . At low Pe , swimming is only worthwhile if the movement is toward regions of higher solute concentration.

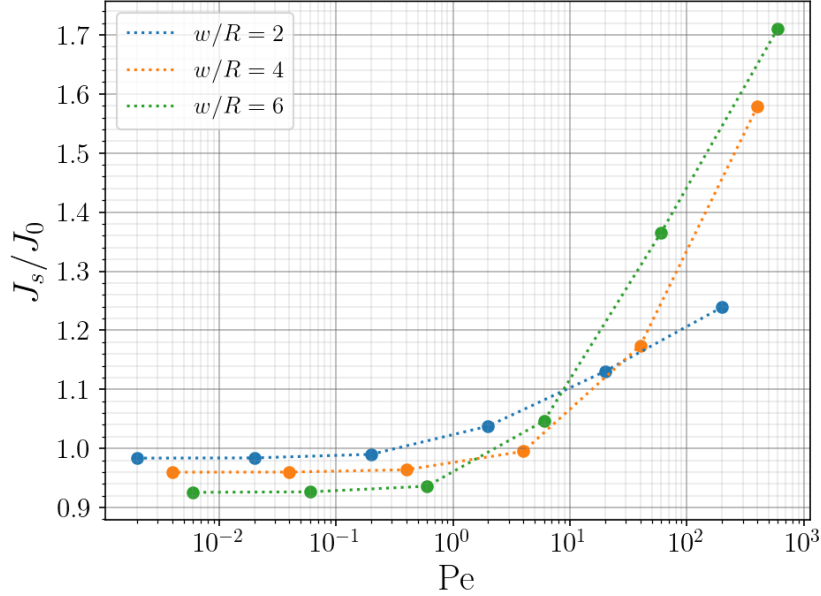


Figure 3. Sherwood number as a function of Pe considering $W/R = 10$ for $w/R = 2, 4$ and 6 .

4 Maximizing solute intake in a concentration gradient

The fluid-solid interaction process, performed by the ambient fluid and the rectilinear swimmer, can be decomposed in a sequence of *actions* (activation of one arm) made by the *agent* (swimmer) that receives a *reward* by achieving different *states*. The four possible states s_t , at time t , for our three-sphere swimmers are: both arms contracted (state 1), left arm contracted and right arm extended (state 2), left arm extended and right arm contracted (state 3) and both arms extended (state 4). When the swimmer activates only one arm per unit time, the sequence of states 4-2-1-3-4-2... produces the swimming gait to the right as shown in Fig. 2. The two possible actions a_t are to activate either left (action 1) or right (action 2) arm of the swimmer.

We consider here the reward that we denote as *intake increase*, based on the interaction among the swimmer, the fluid and the solute concentration field along the time interval $[t, t + 1]$:

$$r_{t+1} = J(t + 1) - J(t). \quad (10)$$

The *learning problem* we pose here is to determine a *policy* (that is, a strategy to choose actions) such that the *total reward* $R = \sum_{t>0} \gamma^t r_t$ is maximized, where $0 < \gamma \leq 1$ is a discount factor.

We focus in the case of a swimmer with $W/R = 10$ and $w/R = 6$, surrounded by a solute concentration field that is always 0 at its surface and, at time $t = 0$, has reached its steady state with value $C_\infty(x, y, z) = gx$ far from the agent. The presence of a far-field gradient $g > 0$ makes that the best policy is the sequence of actions that makes the swimmer to translate to the right, that we have called the swimming gait. A learning process is considered as successful if the swimming gait is learned, and a failure otherwise.

As for the learning algorithm, we adopt *Q-learning*. An action-value matrix $Q(s, a)$ (initialized as a zero-matrix, for example) is updated by means of the *experience* gained by the agent, this is, the 4-tuple $(s_t, a_t, s_{t+1}, r_{t+1})$, for each t . The updating rule is given by

$$Q_{t+1}(s_t, a_t) = (1 - \alpha)Q_t(s_t, a_t) + \alpha \left(r_{t+1} + \gamma \max_{a \in \{1,2\}} Q_t(s_{t+1}, a) \right), \quad (11)$$

where α is the *learning rate* and $\gamma \in (0, 1)$ is the discount factor. After the N updates, one obtains matrix Q_N , which converges as $N \rightarrow +\infty$ to a solution of the Bellman optimality equation.

In these experiments we adopt *off-policy learning*. A large sequence of randomly selected actions is simulated so as to generate and store a list of *experiences*. We use a time step of $\delta t = 0.1$ and a spatial resolution ensuring that the mesh size close to the spheres is about $0.05R$.

Once the experience database is generated, Q-learning is repeatedly run with different values of the parameters α and γ on (11), computing the percentage of learning successes in each case. This allows us to generate a heat map on parameter space, such as the one shown in Fig. 4. At $Pe = 0.06$ learning to translate up the concentration gradient shows to be quite “easy”, in the sense that for most of the parameters one gets very high success rates.

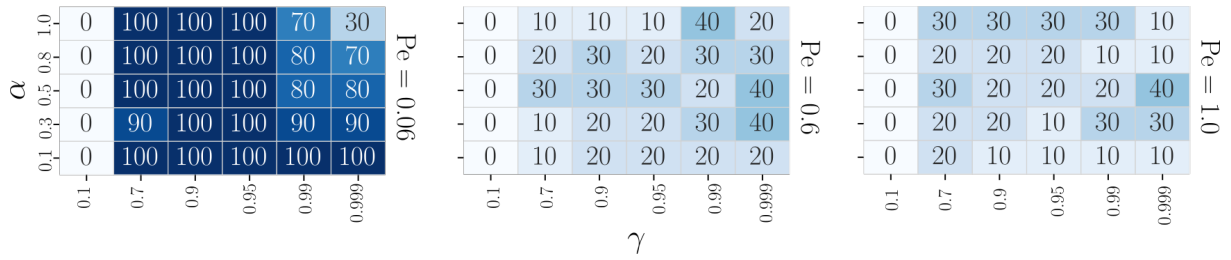


Figure 4. Heat maps of percentage of learning success obtained from 10 sets of 500 consecutive experiences for the data sets corresponding to $Pe = 0.06, 0.6, 1$.

However, the success rate falls significantly as soon as Pe is increased toward 1. This is not surprising, since the surrounding concentration field is a *dynamic environment* with high dimensionality of which the agent has very little information.

Future work is aimed at studying *state augmentation*, i.e., incorporate into the definition of the states additional quantities, which can be seen as coming from simulated sensors. Comparing heat maps of different augmented states provides us with a measure of the *efficiency* of each possible sensor.

5 Active learning at high Péclet number

When Pe is high, it is possible to significantly increase the solute flux simply by swimming, so as to move away from the region already depleted by the swimmer. We have seen this effect quantitatively for the three-sphere swimmer, but it is valid in most models.

We thus turn to a different learning problem: Given a swimmer in a homogeneous concentration field, at a Pe number such that significant increase in the solute flux can be achieved by translation, is it possible to learn an effective gait by active Q-learning?

To consider a different swimmer geometry, let us study an articulated swimmer made of 4 elliptic bodies whose joints can rotate between a maximum and a minimum angle. The swimmer moves throughout an ambient fluid with solute concentration such that $C = C_\infty$ far from it. The initial condition for the transport problem is given by the corresponding steady state on the problem (7)-(8) for a random initial posture of the swimmer. An action performed by swimmer consist in the activation of one arm per unit time, this is, if the arm is in position of minimum angle, then, the activation will lead it to the maximum angle position.

In Fig. 5 we present the instant solute flux towards the 4-body articulated swimmer at high Pe ($Pe > 100$) during one realization of the Q-learning process with $\gamma = 0.8$ and $\alpha = 1.0$, compared against the flux perceived by the swimmer when the actions are selected in a pure random fashion. The fluxes were normalized by the flux at the initial condition. The reward used in this case was the intake increase *restricted to the first elliptic body* of the swimmer (the head). The agent learns on-line, namely, it selects each action according to a policy that depends on Q_t . Preference is given for a_{t+1} to be taken as the maximum over a of $Q_t(s_{t+1}, a)$. One expects that, as time evolves, Q_t incorporates previous experiences and thus encodes a policy that (approximately) maximizes the reward.

The results show that the agent indeed learns a policy that significantly increases its instantaneous flux. In fact, it quadruplicates it after just 2000 learning steps. It manages to do so by translating in the general direction of the swimmer's head, as can be seen in Fig. 6. In this way, the agent leaves a depleted wake behind it and the head is always exposed to "fresh" solute. Comparatively, the stirring effect of performing random motions, with no net average displacement, only increases the flux by less than 50%.

6 Conclusions

The work described in this article is mainly of exploratory nature. We have shown that it is possible to create a simulation environment with accurate geometrical and physical representation of microswimmers that is suitable for its application in learning problems that involve the surrounding concentration field. With moderate discretization in both time and space, the simulated environment leads to learned policies that are physically meaningful. Future work concerns the application of the methodology to identify optimal policies for different swimmer/environment models. For efficient computation, combinations of discretization and learning strategies that minimize cost will be investigated.

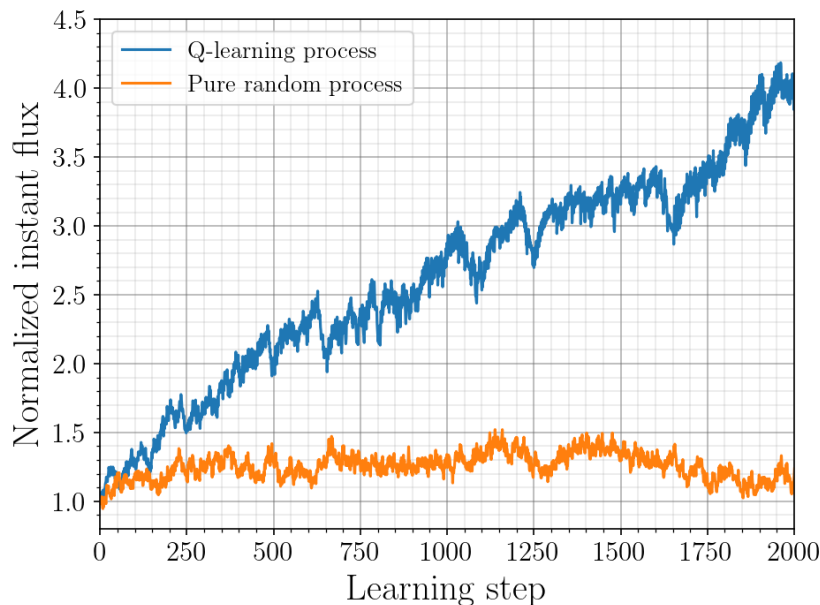


Figure 5. Solute flux towards the head of the swimmer normalized by the flux at time $t = 0$. In blue the active Q-learning process, in orange a totally random action-selection policy.

Acknowledgements. The authors gratefully acknowledge the financial support received from the São Paulo Research Foundation FAPESP/CEPID/CeMEAI grant 2013/07375-0, and from Brazilian National Council for Scientific and Technological Development CNPq grants 305599/2017-8 and 310990/2019-0. This research was carried out using computational resources from the Cluster-Sala Jürgen Tischer, Department of Mathematics, Universidad del Valle, Cali, Colombia. The authors are thankful to the developers of the free and open source software used for this publication.

Authorship statement. The authors hereby confirm that they are the sole liable persons responsible for the authorship of this work, and that all material that has been herein included as part of the present paper is either the property (and authorship) of the authors, or has the permission of the owners to be included here.

References

- [1] G. I. Taylor. Analysis of the swimming of microscopic organisms. *Proceedings of the Royal Society of London. Series A. Mathematical and Physical Sciences*, vol. 209, n. 1099, pp. 447–461, 1951.
- [2] J. Lighthill. Flagellar hydrodynamics. *SIAM review*, vol. 18, n. 2, pp. 161–230, 1976.
- [3] E. M. Purcell. Life at low reynolds number. *American Journal of Physics*, vol. 45, n. 1, pp. 3–11, 1977.
- [4] J. Elgeti, R. G. Winkler, and G. Gompper. Physics of microswimmers—single particle motion and collective behavior: a review. *Reports on Progress in Physics*, vol. 78, n. 5, pp. 056601, 2015.
- [5] E. Lauga. Bacterial hydrodynamics. *Annual Review of Fluid Mechanics*, vol. 48, pp. 105–130, 2016.
- [6] R. E. Goldstein. Green algae as model organisms for biological fluid dynamics. *Annual Review of Fluid Mechanics*, vol. 47, pp. 343–375, 2015.
- [7] R. E. Goldstein. Batchelor prize lecture fluid dynamics at the scale of the cell. *Journal of Fluid Mechanics*, vol. 807, pp. 1–39, 2016.
- [8] M. Lighthill. On the squirming motion of nearly spherical deformable bodies through liquids at very small Reynolds numbers. *Communications on Pure and Applied Mathematics*, vol. 5, n. 2, pp. 109–118, 1952.
- [9] J. Blake. A spherical envelope approach to ciliary propulsion. *Journal of Fluid Mechanics*, vol. 46, n. 1, pp. 199–208, 1971.
- [10] V. Magar, T. Goto, and T. J. Pedley. Nutrient uptake by a self-propelled steady squirmer. *The Quarterly Journal of Mechanics and Applied Mathematics*, vol. 56, n. 1, pp. 65–91, 2003.
- [11] V. Magar and T. J. Pedley. Average nutrient uptake by a self-propelled unsteady squirmer. *Journal of fluid mechanics*, vol. 539, pp. 93–112, 2005.
- [12] A. Najafi and R. Golestanian. Simple swimmer at low reynolds number: Three linked spheres. *Physical Review E*, vol. 69, n. 6, pp. 062901, 2004.

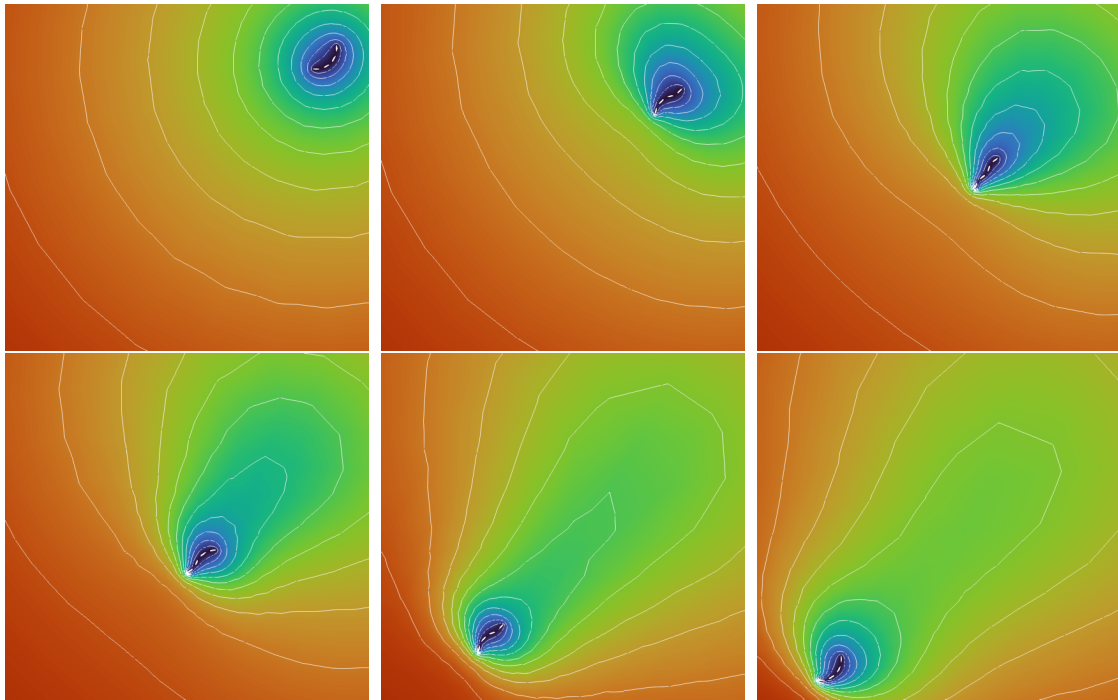


Figure 6. Solute concentration around the swimmer at different times.

- [13] A. Najafi and R. Golestanian. Propulsion at low Reynolds number. *Journal of Physics: Condensed Matter*, vol. 17, n. 14, pp. S1203, 2005.
- [14] B. Nasouri, A. Vilfan, and R. Golestanian. Efficiency limits of the three-sphere swimmer. *Physical Review Fluids*, vol. 4, n. 7, pp. 073101, 2019.
- [15] L. Berti. *Numerical methods and optimisation for micro-swimming*. PhD thesis, Université de Strasbourg, 2021.
- [16] O. S. Pak, E. Lauga, C. Duprat, and H. Stone. *Theoretical models of low-Reynolds-number locomotion*. Royal Society of Chemistry, 2015.
- [17] N. Cohen and J. Boyle. Swimming at low Reynolds number: a beginner's guide to undulatory locomotion. *Contemporary Physics*, vol. 51, pp. 103–123, 2010.
- [18] Q. Wang and H. Othmer. Analysis of a model microswimmer with applications to blebbing cells and mini-robots. *J. Math. Biol.*, vol. 76, pp. 1699–1763, 2018.
- [19] M. S. Alnæs, J. Blechta, J. Hake, A. Johansson, B. Kehlet, A. Logg, C. Richardson, J. Ring, M. E. Rognes, and G. N. Wells. The fenics project version 1.5. *Archive of Numerical Software*, vol. 3, n. 100, 2015.
- [20] S. Paz and G. C. Buscaglia. Simulating squirmers with volumetric solvers. *Journal of the Brazilian Society of Mechanical Sciences and Engineering*, vol. 42, n. 10, pp. 1–27, 2020.
- [21] R. F. Ausas, C. G. Gebhardt, and G. C. Buscaglia. A finite element method for simulating soft active non-shearable rods immersed in generalized newtonian fluids. *Communications in Nonlinear Science and Numerical Simulation*, vol. 108, pp. 106213, 2022.
- [22] D. Tam and A. Hosoi. Optimal feeding and swimming gaits of biflagellated organisms. *Proceedings of the National Academy of Sciences*, vol. 108, n. 3, pp. 1001–1006, 2011.
- [23] F. Alouges. Low Reynolds number swimming and controllability. *ESAIM Proceedings*, vol. 41, pp. 1–14, 2013.